Eur. Phys. J. D **15**, 321–329 (2001)

THE EUROPEAN PHYSICAL JOURNAL D

EDP Sciences

Computed orientational anisotropy and vibrational couplings for the LiH + H interaction potential

E. Bodo[1], F.A. Gianturco[1,a], R. Martinazzo[2], and M. Raimondi[2]

[1] Department of Chemistry, The University of Rome, Citta' Universitaria, 00185 Rome, Italy
[2] Department of Physical Chemistry and Electro-chemistry, University of Milan, and CNR Center CSRSRC, via Golgi 19, 20133 Milan, Italy

Received 16 February 2001 and Received in final form 23 May 2001

Abstract. The interaction between LiH and H has been calculated using a Coupled Cluster approach in view of examining the strength of the coupling between the impinging atom and the rovibrational LiH states in low energy collision regimes. The potential energy surface was thus obtained by considering not only the angular anisotropy but also the dependence of the interaction energy on the vibrational motion of the LiH molecule, hence producing the strength of the vibrational coupling. The main objective is that of gaining a realistic description of the interaction in the sub-reactive region. The results of our calculations show here that this interaction should be used in conjunction with that of the reactive configurational space because of the strong coupling between the non-reactive and the reactive channels in the present system makes the full reactive scattering calculations a more reliable way to obtain realistic cross-sections also for inelastic relaxation and excitation processes.

PACS. 34.20.-b Interatomic and intermolecular potentials and forces, potential energy surfaces for collisions – 34.20.Gj Intermolecular and atom-molecule potentials and forces – 34.50.-s Scattering of atoms and molecules

1 Introduction

The dynamical and reactive processes involving LiH/LiH^+ molecules have received a great deal of attention from our group in the last 5 years [1–4] because of their relevance as one of the possible cooling agents of the protostructures that are supposed to exist in the primordial universe [5,6]. The understanding of the reactive behaviour of the LiH species is important in establishing the abundance of the molecule in the universe and, thus, its relevance for its radiative cooling processes. On the other hand, the last processes are controlled by the inelastic collisions with the most abundant atoms like H/H^+, D/D^+, He/He^+, which can excite the molecular species into low-lying rotovibrational states and thus allow them to radiatively remove the excess energy of a collapsing cloud.

The reactive and the non-reactive processes between the simple atoms mentioned above and the molecular species containing such atoms (H_2/HD, H_2^+/HD^+, HeH^+, LiH/LiH^+) are usually very entangled. For the title molecule, with the exception of the chemically inactive He atoms [2,7–9], one should consider the full dynamical reactive problem and extract from it the relevant cross-sections. In general, the actual implementation of this procedure is still not straightforward today because of the huge number of accurate *ab initio* points necessary to obtain a reliable interaction potential and because exact reactive scattering calculations are only feasible for the low partial waves. In some cases one limits oneself with the acquisition of less detailed information and the application of *exact* and *direct* methods to the calculation of the rate constants becomes feasible as shown by Miller (*e.g.* [10]). In other cases one has to resort to some approximate scheme and try to extract dynamical information from "constrained" scattering calculations. In some situations, for example, one can exclude the presence of reactive channels (both closed and open) if they happen to be hindered by classically forbidden regions with small tunnelling probabilities.

For the LiH + H system we have already looked at the reaction forming H_2 in the constrained collinear geometry [9], computing the relevant Potential Energy Surface (PES) and following the dynamics by means of classical and quantum (time-dependent) methods. The main result was the small tendency for the reaction to occur, although it showed an high exoergicity and the potential energy did not indicate an appreciable activation barrier in the route to the products: only for small values of the translational energy and almost independently of the initial vibrational level the computed reaction probabilities were thus appreciable. This behaviour has been ascribed to the topological

[a] e-mail: fagiant@caspur.it

properties of the H_2 exit channel which appears to prevent the high energy "trajectories" to go into the formation of products. Subsequently, Lee *et al.* [11] have computed the PESs for the lower-lying electronic states of the LiH_2 system, looking at a large number of collinear, C_{2v} and C_s geometrical forms in the reactive configurational subspace. The authors of [11] were particularly interested in the photochemical processes that can occur between excited lithium atoms and the hydrogen molecule. One feature of possible interest for the LiH dynamics in the presence of the H atom was the suggested formation of the excited Li($2p$) atom *via* a non-adiabatic transition to the first electronic excited state of the system, where the $H_2(n = 0)$ + Li channel opens at 1 624 cm^{-1} of collision energy above the LiH($n = 0$) + H fragments. Even if we are not interested in such a complicated process an exact study of the dynamical behaviour of the present system should take this fact into account.

In this work we supplement the available data on the interaction potential of the title system with an analysis of the sub-reactive configurational space. This is done by looking at the full angular dependence of the potential LiH−H for several values of the internuclear distance of the diatomic molecule chosen to start at the bottom of its potential curve. This study is specifically intended to provide a fuller understanding of the interaction acting during the LiH + H scattering process. In particular, we already know that on the "H side" the interaction opens the way to the products Li + H_2 but we do not know anything as yet on what happens when the projectile atom approaches the molecule outside a small angular cone around the H atom. Indeed, from a dynamical point of view the reaction forming H_2 could turn out to be a rather rare event either because the "dynamical" constraints in the favorable quasi-collinear arrangements [9] or because of the unfavorable approaching angle of the projectile. If this were the case, the elastic and the inelastic processes between LiH and the most abundant H atom would dominate the scattering outcome, although we will see below that the correct transition probabilities can only come from fuller reactive scattering calculations.

In the following, we will first briefly examine the method employed to obtain the interaction potential while in Section 3 we will analyze in detail the features of this interaction in terms of the rotational anisotropy and vibrational coupling. In Section 4 we will use the interaction potential in a non-reactive scattering calculation as a numerical test done in order to gain some insight into the dynamical behaviour. This test can be useful as a guidance for further, more exact, dynamical studies of the system. The present conclusions are given in Section 5.

2 The computational method

The potential energy surface was calculated on a dense grid for the three Jacobi coordinates defined, as usual, as: R the distance between the center of mass of the diatom (taken to be composed of the ^{7}Li isotope) and the impinging atom, r the internuclear distance of the diatom and θ the angle between them, taken to be 0 for the Li−H−H linear configuration. The grid was a regular one and consisted of 44 points in R (from 1 to $11.75a_0$), 14 in θ (from 0 to 180 degrees) and 5 points in r ($r_1 ... r_5$). We set r_1 and r_5 to the vibrational turning points of the $v = 4$ vibrational level; *i.e.* $2.29364a_0$ and $4.30473a_0$ respectively; for r_3 we used the ground-state equilibrium bond length, $3.01392a_0$. The two remaining values were chosen as $r_2 = (r_1 + r_3)/2$ and the $r_4 = (r_3 + r_5)/2$, *i.e.* $2.65378a_0$ and $3.65932a_0$.

We employed the Coupled Cluster method [12] as implemented in the standard suite of programs GAUSSIAN-98 [13]. We explicitly correlated 3 electrons, the two core electrons of the Li atom being fixed in the SCF molecular orbital. We used all the SCF-MO vectors, considering all single, all double and triple excited configuration out of the SCF reference function, according to the SD(T) Coupled-Cluster method. The results are in very good agreement with FullCI calculations with the same basis-set and the same number of active electrons. The inclusion of the core correlation increases the computational cost of the calculation without any substantial change of the interaction energy in the configurational region relevant for low energy processes. This has been checked for the equilibrium distance of the diatomics by computing the potential along a direction of approach of the H atom on the Li side of the molecule, where we expect the core correlation to have its greatest role.

The basis-set used was a standard atom-centered basis set of contracted Gaussian type orbitals, the $6-311+(3df, 3pd)$ one. We checked the calculated energies against those obtained with a basis-set consisting of cc-pV4Z functions for Li plus aug-cc-pVTZ functions for H. Once again we considered the same test orientation mentioned above and did not note any appreciable change in the results. The chosen basis set doesn't lead to an appreciable Basis Set Superposition Error (BSSE) for the mentioned direction of approach, where once again we expect to have the greatest error. We estimated this error with the standard Counterpoise correction method of Boys and Bernardi [14]. We therefore decided to neglect this correction for all the geometries considered.

3 The interaction

As usual, the interaction energy was calculated as $V^{\rm int}(r, R, \theta) = V(r, R, \theta) - E_{\rm H} - V_{\rm LiH}(r)$ for all the *ab initio* points. In this section, after noting some general features of the interaction, we will discuss the orientational anisotropy of the Rigid Rotor (RR) surface, that is the surface with r fixed at its equilibrium value which is here labelled as r_3. Since, usually, this kind of surface governs, to a good approximation, the vibrationally elastic dynamics such orientational anisotropy is relevant for the angular momentum dynamical coupling. Later on we will further discuss some properties of the vibrational coupling along with some problems encountered in their numerical evaluation which chiefly arise from the strong interaction that we found here to exist between the two partners.

Table 1. Computed minima for each of the 5 PESs. The distances in the first column are the HH distances. The energies in the last column are given with respect to the energy of the isolated partners with $r_{\mathrm{LiH}} = r_{\mathrm{e}}$.

	d_{HH}/Å	E/a.u.	ΔE/eV
r_1	0.7073	−8.547957	−0.712
r_2	0.7092	−8.571576	−1.356
r_3	0.7521	−8.585220	−1.727
r_4	0.7318	−8.594664	−1.984
r_5	0.7153	−8.597774	−2.068

The computed absolute minimum of the surfaces was found to correspond to a geometry in which the approaching angle of the impinging H atom is ∼20°, the internuclear diatomic distance is the largest distance used and the value of R is such that the distance between the two hydrogen atoms is to a good approximation the internuclear distance of the H_2 molecule (0.741 Å as quoted in [15]). The bottom of the well is 2.068 eV below the LiH(r_3) + H asymptote. This value compares quite well with the exoergicity of the reaction (ΔE = 2.195 eV is the value computed without ZPE from the spectroscopic data of Refs. [15,16]), showing that this well is the entrance of the *valley* corresponding to the outgoing channel in which we form the products of the reaction H_2 + Li [9,11]. When we look at the corresponding minima for each surface at fixed r (see Tab. 1) we have very similar results for the largest values of the diatomic distance. This means that the H_2 channel is almost flat, *i.e.* its energy content depends very little on the LiH distance. This is clearly due to the fact that, qualitatively, the Li + H_2 fragments interacts only by means of the short-range chemical forces: apart from the weak van der Waals forces, in fact, the interaction of the last two fragments mainly arises from the re-coupling between the valence Li electron and one of those in the hydrogen molecule, a process which occurs within a rather small interval of the relevant distance, as already noted for the collinear arrangement [9]. On the other side of the target (the Li side) the surfaces with $r \leq r_3$ show only a small, outermost well which is clearly due to the dipole-induced dipole and the dispersion terms. For greater values of r, thanks to the very short-range character of the three body non-additive contribution in this system, we observe a situation very close to an asymptotic one: when the diatomic distance is very large the rigid-rotor surfaces usually show wells which are close to the target atoms, corresponding to the formation of the relevant diatomic molecules. In our case we already observe such a behaviour for values of r slightly greater than the equilibrium: two wells appear in the surface, one located near the target hydrogen atom corresponding to the formation of H_2 and the other one near the Li atom corresponding to the formation of an LiH molecule in which the H atom comes from the projectile (*i.e.* we observe the exit channel of the hydrogen exchange reaction).

This situation is clearly illustrated in Figure 1, where we report a tridimensional view of the interaction for

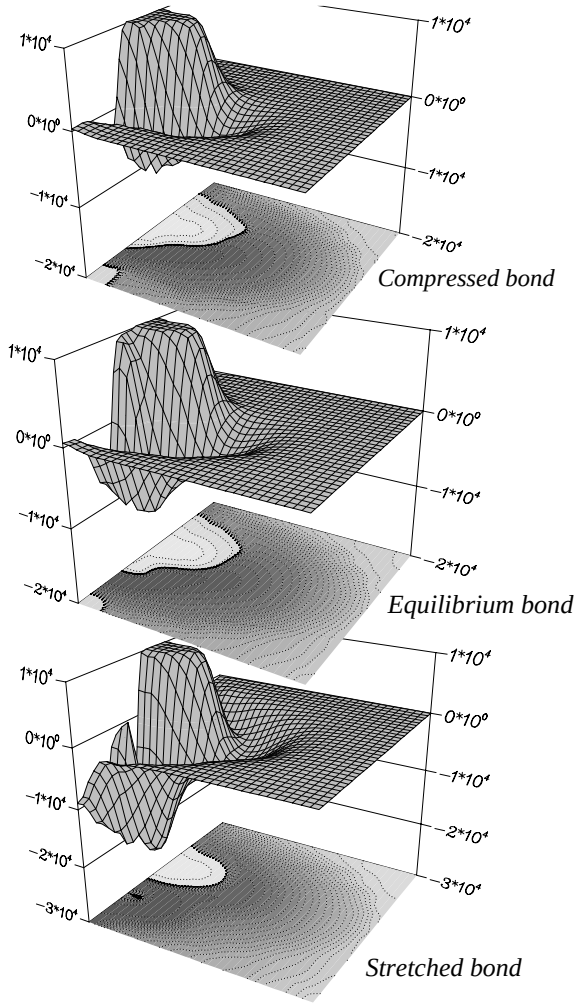

Fig. 1. 3D view of the effect of the stretching the LiH bond on the potential energy surface. The distances of the diatomic partner are (from top to bottom) 2.29, 3.014 and 4.30 a.u. The plots are given in polar coordinates, using the familiar Jacobi R and θ. The values of R are within 1 and 6 a.u. The interaction energy is reported in cm^{-1}.

a compressed (top panel, $r = r_1$), equilibrium (middle panel, $r = r_3$) and elongated (lower panel $r = r_5$) LiH bond. The coordinates chosen are the Cartesian coordinates of the projectile, *i.e.* $x = R\cos\theta$ and $y = R\sin\theta$, where R and θ are the usual Jacobi coordinates. For each value of r the surface is represented around the LiH center of mass and for values of R not greater than 6 a.u. The actual position of the target atoms can be identified by the position of the repulsive core in the middle of each surface; when the diatomic distance becomes sufficiently great the two peaks due to the repulsion between the target atoms and the projectile become very distinct. All the features mentioned above are clearly visible: one deep well on the H side of the target for all values of r and one less deep well on the Li side when the diatom is stretched. It should be noted that the three surfaces differ in their asymptotic value (LiH(r_i) + H); this is why for the largest diatomic distance we observe a much deeper

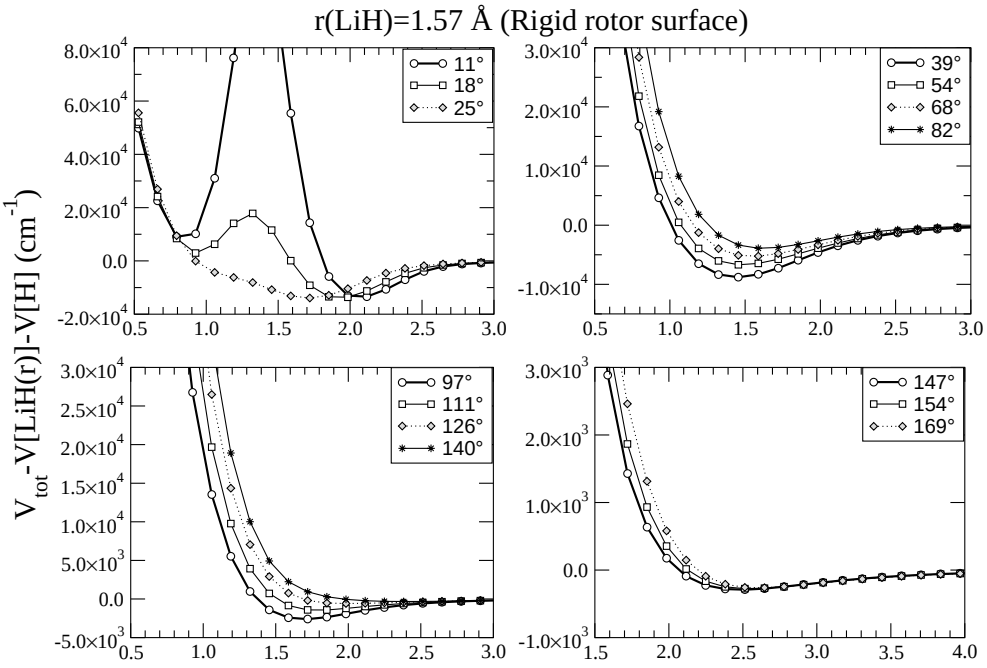

Fig. 2. The rigid rotor surface plotted along several angular cuts as a function of R. The R values are in a.u.

well in the *interaction* potential. When considered on a total energy scale the minimum energies in the last two surfaces reported compare quite well, *i.e.* the exit channel of the reaction forming H_2 is, as already mentioned, almost flat in energy (see Tab. 1).

3.1 The orientational anisotropy

The RR surface that we have mentioned earlier is plotted along several of its monodimensional cuts in Figure 2, as a function of R, for fixed values of the orientational angle θ. As it is evident from the upper-left panel, the surface shows a prominent cusp due to the nuclear-nuclear repulsion terms in the Hamiltonian between the two hydrogen atoms. The cusp is, indeed, localized in the region where the impinging H atom approaches directly the H side of the LiH molecule. Apart from the cusp region, however, the behavior of the surface is fairly smooth and the main structural feature appears to be that of a weakening of the interaction when changing the direction of approach of the H atom towards the Li end of the molecule. This trend is confirmed when one looks at the interaction energy as a function of θ as reported in Figures 3 and 4. The first of the two figures shows what happens for the R values where we find the greater variation along the θ coordinate: the cusp (evident for $\theta = 0°$) disappears for $\theta \sim 20°$, to be replaced by a deep minimum for the orientations between 20° and 50°. This minimum is then seen to be pushed outwards by the Li atom, thereby making the potential energy surface become repulsive in the large-angle region of interaction. The next figure shows the same picture but for R values taken in the long range region of the potential: here the behavior is smoother and the potential is always attractive because of the dispersion energy contributions included by the dynamical correlation. In both the last two figures we have also reported (lower panels) the derivative of the interaction potential with respect of the orientational variable. This quantity represents the classical torque acting on the colliding system and can be considered to be a measure of the strength of the rotational coupling acting on the target during the scattering event. Quantum mechanically, the orientational anisotropy is commonly expressed in terms of the multipolar expansion of the interaction potential $V(R,\theta) = \sum_\lambda V_\lambda(R) P_\lambda(\cos\theta)$. Some of the computed V_λ terms are shown in Figure 5. As is evident from the figure, all the terms show the cusp peak arising from the very localized repulsion between the two HH atoms, which can be hardly represented by a rapidly converging Legendre series; also note in this context that, since R is almost equal to the distance between Li and the projectile atom, the peak appears at a distance close to r_3. Apart form this peak, the deep HH well is well described by the first few terms and therefore for $R > r_3$ the series converges more rapidly.

3.2 The vibrational coupling

One usually describes the coupling between the translational and the vibrational motion in a non-reactive collision by computing the matrix elements of the interaction potential over the vibrational states of the target molecule. Although in the present case, owing to the presence of the reactive channels, such description could not be appropriate any more we can still obtain some information on the role of the vibrational motion when the two fragments are far apart, as we shall discuss below.

When calculating the vibrational couplings that exist for strongly interacting systems an important source of errors can be the incorrect evaluation of the vibrational

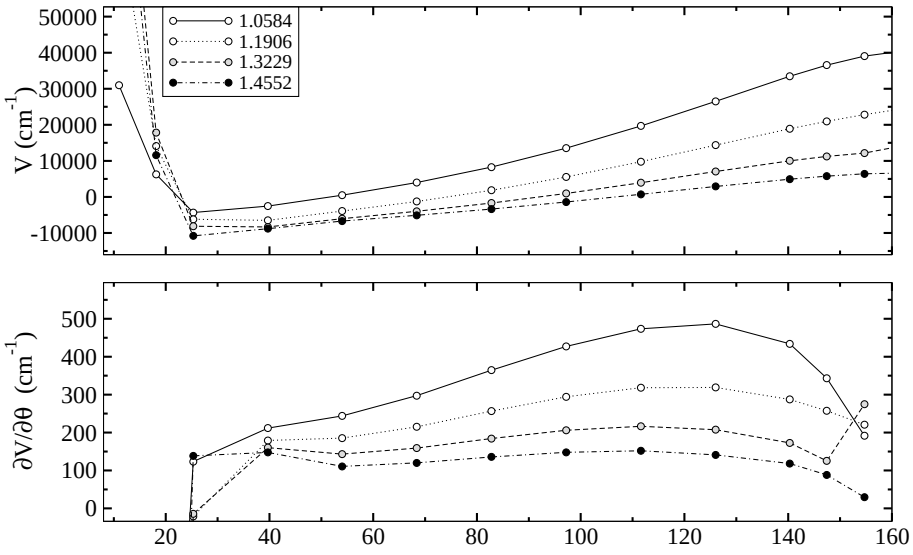

Fig. 3. Upper part: rigid rotor interaction potential as a function of θ for selected values of R (indicated in a.u.). Lower: first derivative of the potential with respect to θ.

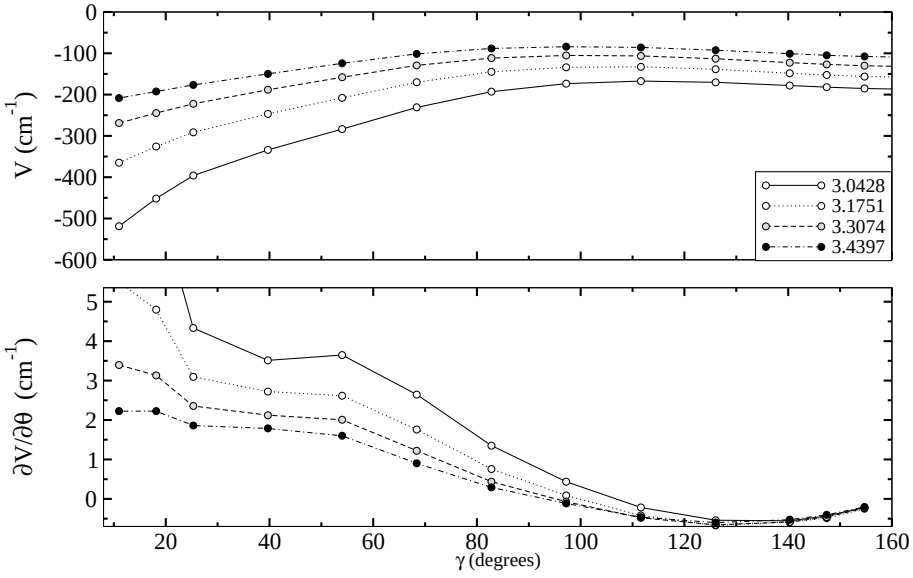

Fig. 4. Same as in Figure 5, but for larger R values.

matrix elements because of the limited portion of the r region which is being considered when computing the surface. This can be simply understood by considering some "rigid" model potential

$$V(r, R, \theta) = V(r_{\rm eq}, R, \theta) \tag{1}$$

for which the off-diagonal vibrational couplings should vanish:

$$V_{n'n}(R, \vartheta) = V^{\rm int}(r_{\rm eq,} R, \vartheta)\, \langle n'|n\rangle \cdot \tag{2}$$

In the numerical computation of this expression the off-diagonal coupling elements may turn out to still remain quite large for strongly interacting systems if the vibrational integration is not performed over a sufficiently large radial range, especially for high Δn transitions, because of the "overlap" error in the truncated r region. To overcome this problem, we used an r extrapolation of the interaction potential, both in the large-r region and in the small-r region and made sure to apply it over the whole grid of R, θ points employed to get the full interaction.

For the large-r region we took advantage of the fact that, as the non-additive three body contribution goes rapidly to zero, the interaction potential of the AB-C system becomes a sum of two-body potentials $V_{\rm AC}$ and $V_{\rm BC}$. Since the BC distance depends on r as

$$r^2_{\rm BC} \sim \left(\frac{\mu}{m_{\rm B}} r\right)^2 [1 + O(R/r)] \tag{3}$$

(similarly the AC distance) the shape of the interaction potential in the limit $r/R \to \infty$ is determined by the long-range behavior of the diatomic AC and BC potentials. Therefore, we decided to extrapolate the interaction with the simple functional form

$$V(r, R, \theta) = \frac{A(R, \theta)}{r^n} + \frac{B(R, \theta)}{r^m} \tag{4}$$

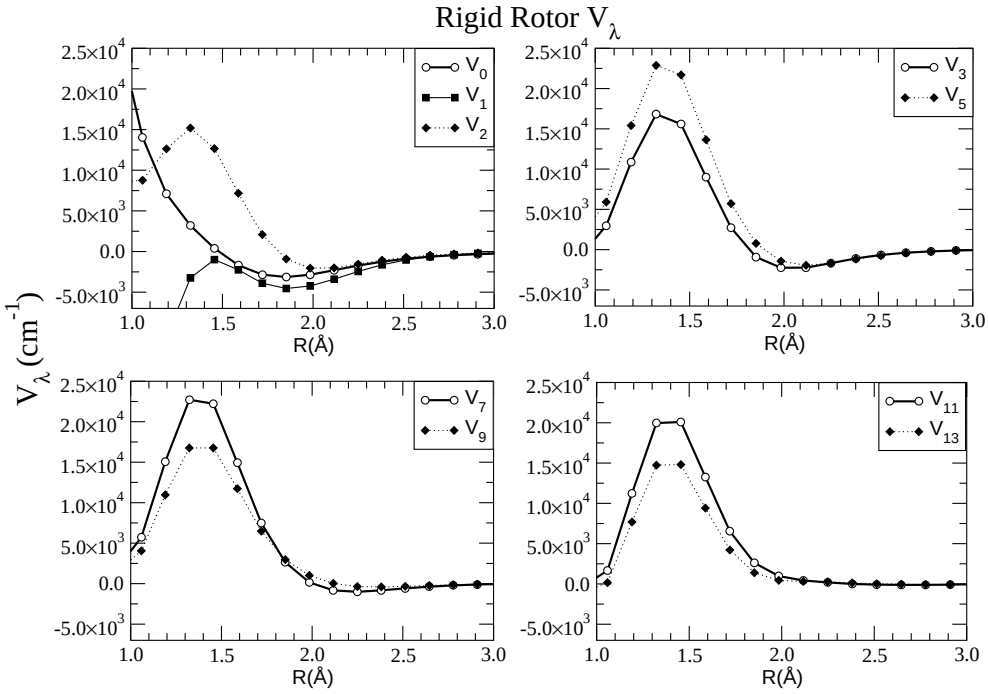

Fig. 5. Selected terms of the multi-polar expansion of the rigid rotor potential as a function of R.

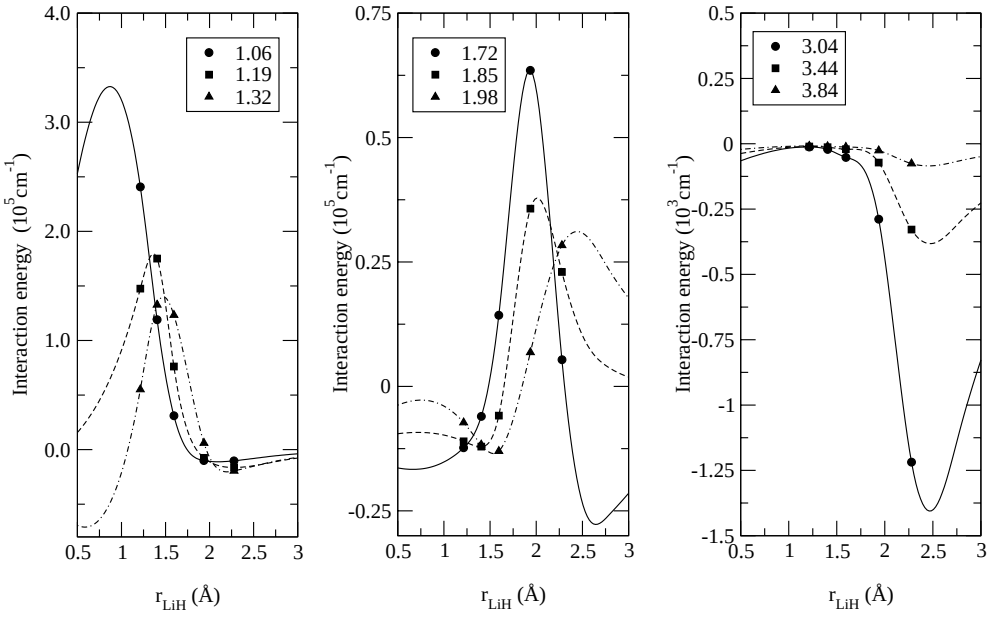

Fig. 6. Cuts of the full potential energy surface along the r coordinate. These cuts are taken for the same angle θ and for different values of the R coordinate.

where the A and B coefficients are determined by ensuring a smooth joining *via* a B-spline of the computed points of r for each (R, ϑ) set. We chose $n = 6$ and $m = 8$ because the diatomic limits involved in our case are LiH and HH.

On the other hand, for $r \to 0$ we recognize that the interaction potential simply reduces to the diatomic interaction potential of the system made by our projectile and the united-atom AB:

$$V^{\text{int}}(0, R, \vartheta) = V_{\text{U-C}}(R) \tag{5}$$

where U denotes the united atom AB, as can be easily seen starting from the definition of V^{int}. Therefore, for each couplet of (R, ϑ) values, we add a new point at $r = 0$ that results from the UC interaction potential (in our case BeH). The extrapolation is performed by using a B-spline over this "enlarged" set of r points.

This overall procedure turns out to be good for our purposes, providing us with a smooth, well behaved $V(r)$ curve for each (R, ϑ) point. This is shown in Figure 6 where we report the computed and fitted data points as a function of r for selected values R and at fixed value of $\theta = 11.0$ (*i.e.* on the H side of the target). We show the short-range regions in the left and center panels and the long range region in the right panel. Note how well the cusp is reproduced by the fitting procedure both in the inner and in the outer extrapolation regions: it regularly

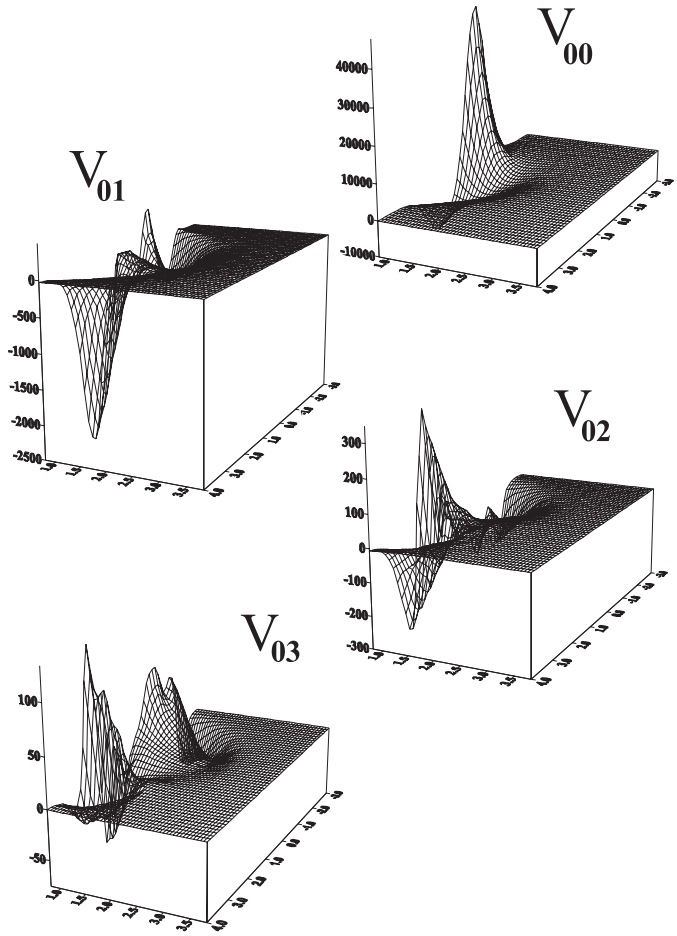

Fig. 7. A 3D view of some of the vibrational couplings (cm^{-1}) in a Cartesian grid with $x = R\cos\theta$ (0.8 Å $\leq x \leq$ 3.8 Å) and $y = R\sin\theta$ (-3.0 Å $\leq y \leq$ 4.0 Å). Four different matrix elements are reported.

moves outward when the R value increases. Clearly, this extrapolation procedure could be very inaccurate if one were interested in high Δn transitions (for which only the computation of the potential is the alternative left), but it gives the correct order of magnitude, *i.e.* without spurious "overlap" terms, of the high Δn couplings. In strongly interacting systems such coupling terms are needed to bring the Close Coupling equations to convergence even for low energy processes, even though their accuracy is not determinant for the cross-sections values.

In Figure 7 we report a 3D view for some of these potential coupling terms in Cartesian coordinates chosen as before ($x = R\cos\theta$, $y = R\sin\theta$). We wish to note the following:

- the vibrationally adiabatic PESs (*i.e.* the diagonal terms) turn out to be, as usual, very similar to the Rigid Rotor surface of Figure 1 (middle panel) described before. Here we have reported the V_{00} term;
- the couplings are dominated by the reactive features of the interaction as evident by the presence of the cusps in the short-range region. However, even in such region they are rather small when compared with the vibrationally adiabatic terms, as can be seen by noting the different scales of the graphs in Figure 7 (see also the middle graph in Fig. 1). This means, as already pointed out before, that even in the reactive regions the potentials is fairly smooth as a function of r (*i.e.* the Li−H distance in the target).We therefore expect that the overall dynamics (reactive and non-reactive) is only weakly influenced by the initial vibrational state of the target molecule, a feature already noted for the collinear arrangement [9];
- apart form the reactive nature of the interaction the marked cusps show the existence of a "light atom" effect, that is of the fact that in a heavy-light molecule the vibrational excitation moves much more the lighter atom and therefore the coupling is largely controlled by the interaction of the latter with the incoming projectile;
- out of the reactive region we observe that the couplings are rather short-ranged in R. This confirms the usual short-range nature of the vibrational excitation-relaxation processes which we have noted many times before (for example [2,17]);
- the couplings tend to converge when the differences between the two vibrational function quantum numbers increase and, more important, the range of action of that coupling also decreases.

4 Dynamical test calculations

Because of the presence of the incipient reaction any attempt to obtain information on the inelastic dynamics cannot leave out the concurrent account of the reactive behaviour of the system. However, since we already know from the collinear reactive calculations [9] that the reaction is "dynamically" hindered by the the narrow exit channel, we can attempt to use the computed rovibrational potential as a model potential in which we artificially close the reactive channels and therefore focus on the sub-reactive dynamics on the newly computed PES. The aim of the present analysis is to obtain some information which could turn out to be of use when more exact dynamical studies of the system will be carried out. We employ the familiar Close-Coupling (CC) approach to solve the rovibrational inelastic problem, for which we defer to the existing literature (for example [18]). The usual starting point is that of choosing the basis functions among those that solve the internal asymptotic Hamiltonians *i.e.* the eigenfunctions of the two isolated fragments. If one makes the assumption that the presence of the (asymptotically closed) dissociative and reactive channels does not alter the dynamics, the only functions one has to consider, in an atom molecule collision, are a finite number of bound states of the molecular target. The basis set is, therefore, constructed from the rovibrational eigenfunctions of the isolated molecule coupled with the angular functions describing the relative rotation of the two fragments in the usual ($JMjl$) representation [18]. The number of basis functions one has to include in the calculation is determined by performing different computational

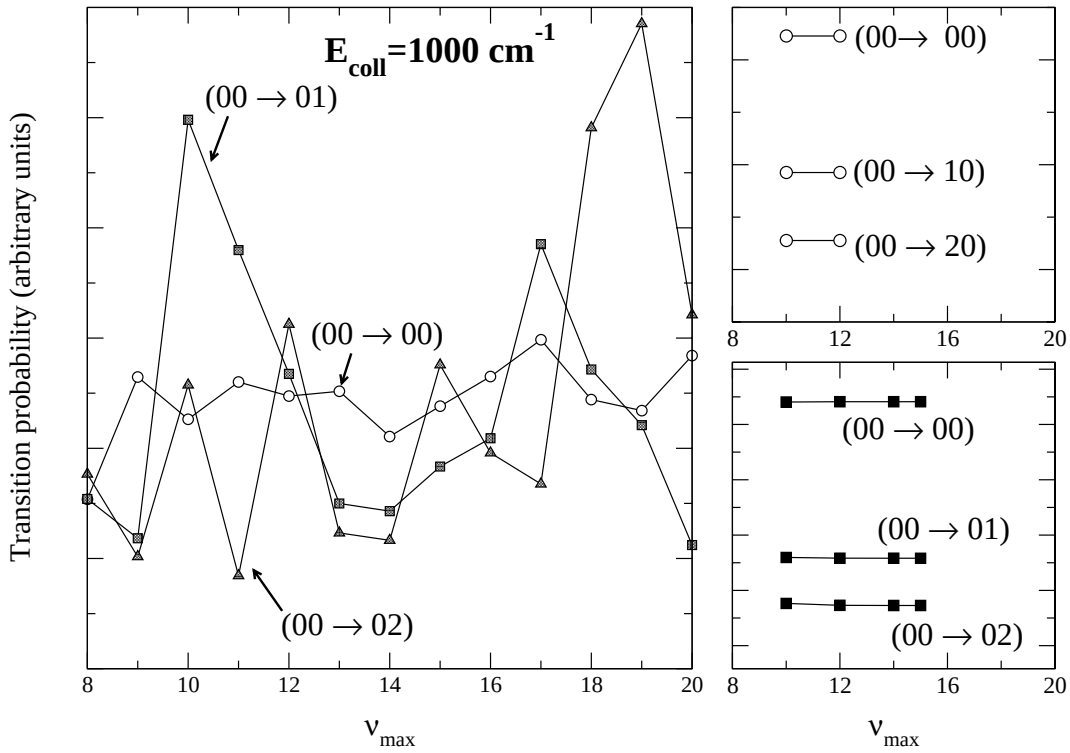

Fig. 8. Test calculations for the S-wave ($J = 0$) partial opacity functions of some ($vj \rightarrow v'j'$) transitions. They are given as a function of the size of the vibrational basis included in the CC equations. Left panel: partial opacity functions between the lowest rotational levels; rotational states up $j_{\max} = 15$ are used for each vibrational level. Lower right panel: same basis as before but with a potential artificially weakened by one order of magnitude. Upper right panel: basis set with only (v, $j = 0$) target functions.

tests and by increasing the rovibrational basis until the requested accuracy in the final, partial and total cross-sections, is reached. Usually, it is sufficient to include some of the closed channels at each defined collision energy to account for the virtual excitations into channels that become *locally* open because of the presence of an attractive potential.

We used the modified log-derivative algorithm of Manolopulos [19] to solve the CC equations; several test calculations have been performed to find the optimum range of integration and the step-size to be used for the propagation of the solution. A number of rovibrational basis of different size has been used in order to obtain convergent calculations with respect to the active asymptotic inelastic subspace. The results of this illustrative example are reported in Figure 8, where the S-wave ($J = 0$) partial opacity functions of the lowest Δj transitions within the ground vibrational manifold are shown. The size of the basis-set has been reported in the abscissa as the number of vibrational manifolds included, each of which contains rotational levels up to $j = 15$. The latter value was chosen such that the total rotational energy implied by the coupled channels is less than the relevant quantum of vibrational energy; higher values of j would need a more appropriate treatment of the target states, that is the calculation of the vibrational couplings with *roto*-vibrational eigenfunctions. The results obtained show, as seen in the left panel of Figure 8 by the three transition curves given as a function of $v_{\max}$, that any attempt to reach convergence of the partial opacities for the *lowest transitions* fails when only bound states of the asymptotic target are considered. This is clearly due to the high degree of local virtual excitation into dissociative eigenstates of the target, that is those additional states which are needed to describe the H_2 fragment in the interaction region whenever the correct dynamics is taken into account through the inclusion of the reaction channels. Indeed, as a simple confirmation of the present analysis we note that the full set of the target rovibrational states is insufficient to span the energy range of the target-projectile interaction. This last consideration explains why the numerical results that one can obtain with the further calculations done as above but using instead a potential coupling that is 10 times weaker (see Fig. 8, lower right panel). In this case, in fact, the convergence is easily reached, for example with sets of calculations including only up to 10 or 12 vibrational levels.

To further explore the effect of the strong interaction on the convergence features we used another fictitious potential matrix which this time did not include the rotational couplings, that is by including only the $j = 0$ component for each of the vibrational channels in the calculations. This model potential matrix corresponds to a spherical potential which only depends upon the diatomic internuclear coordinate. In this case the three test calculations, reported in the upper right panel of Figure 8,

show clearly how it is again possible to reach good numerical convergence with a rather small number of states. This facts clearly indicates the very different role of the rotational and vibrational motions of the target molecule, already noted in the previous analysis of the orientational anisotropy and the vibrational coupling: while the rotational motion is strongly influenced by the potential, because of the orientational character of the reactive interaction, the vibrational motion seems to be less directly coupled by the interaction by rather *via* the anisotropy of the rotational energy ladder.

5 Concluding remarks

In this work we have computed an accurate PES for the LiH + H system and tried to explore the sub-reactive behavior of this fairly simple set of atoms which, however, turn out to constitute a set of strongly interacting partners. The potential, therefore, has to be regarded as an extension to the sub-reactive configurational space of the "reactive" PESs already available [9,11]. This extension becomes necessary in order to obtain from *reactive* scattering calculation accurate values of the transition probabilities both for the reactive and the inelastic collisions. Although such analysis is being planned in our group the computed sub-reactive potential can be used as a model potential in Close-Coupling non-reactive calculations, in which the reactive channel is artificially closed. Such unusual treatment can be of some importance in planning the exact calculations and could be somewhat realistic if one would take advantage of the above mentioned narrowness of the exit channel which imposes a dynamical constraint for the reaction to occur, at least in the favorable collinear geometries [9]. Unfortunately, the strong interaction also found in this instance prevents us from bringing to convergence the calculated partial opacity functions when using only the asymptotic bound states of the target, at least for the lowest partial wave. It is likely that for larger values of the total angular momentum such problem disappears but this is clearly not sufficient to plan the calculations. The relevant dynamical information which can be extracted form these test calculations is the different role played by the rotational and vibrational motions of the target, a feature which can already be inferred by analysing the orientational anisotropy and the vibrational couplings as it was done in Section 3.

The exact calculation of the inelastic transition probabilities for this system by means of a reactive scattering approach still constitute a formidable task. Even if we could compute such probabilities for the lowest partial waves, as it is routinely done today (*e.g.* [20]), the information we are looking for need a much more enlarged set of $J_{\rm tot}$ values to be sampled. Therefore we should try some appropriate approximate scheme that takes into account precisely those properties of the interaction potential that we have described in this work. For example, one may infer that the H_2 configuration should be a configuration of no-return for the system, *i.e.* one may suppose that when the system enters the deep and narrow exit channel of H_2 formation [9] it never comes back on the reagents' side. This would allow one to place an absorbing potential at the bottom of the deep H_2 well in a sub-reactive study whose computational cost would be not much different from a traditional CC calculation. We are currently investigating this and other possibilities for extending the present analysis.

References

1. F.A. Gianturco, P.G. Giorgi, Ap. J. **479**, 560 (1997).
2. E. Bodo, S. Kumar, F. Gianturco, A. Famulari, M. Raimondi, M. Sironi, J. Phys. Chem. A **102**, 9390 (1998).
3. E. Bodo, F. Gianturco, R. Martinazzo, F. Paesani, M. Raimondi, J. Chem. Phys. **113**, 11071 (2000).
4. E. Bodo, F. Gianturco, R. Martinazzo, A. Forni, A. Famulari, M. Raimondi, J. Phys. Chem. A **104**, 11972 (2000).
5. E. Bougleux, D. Galli, Mon. Not. R. Astron. Soc. **288**, 638 (1997).
6. P. Stancil, S. Lepp, A. Dalgarno, Astrophys. J. **458**, 401 (1996).
7. F.A. Gianturco, S. Kumar, S.K. Pathak, M. Raimondi, M. Sironi, Chem. Phys. **215**, 239 (1997).
8. F.A. Gianturco, S. Kumar, S.K. Pathak, M. Raimondi, M.S.J. Gerrat, D. Cooper, Chem. Phys. **215**, 227 (1997).
9. N. Clarke, M. Sironi, M. Raimondi, S. Kumar, F. Gianturco, E. Buonomo, D. Cooper, Chem. Phys. **233**, 9 (1998).
10. W.H. Miller, Faraday Discuss. **110**, 1 (1998).
11. H. Lee, Y.S. Lee, G. Jeung, J. Phys. Chem. A **103**, 11080 (1999).
12. N.S.O.A. Szabo, *Introduction to Advanced Electronic Structure Theory* (Dover Pubns., 1996).
13. M. Frisch, G. Trucks, H. Schlegel, G. Scuseria, M. Robb, J. Cheeseman, V. Zakrzewski Jr., R. Stratmann, J.C. Burant, S. Dapprich, J. Millam, A. Daniels, K.N. Kudin, M. Strain, O. Farkas, J. Tomasi, V. Barone, M. Cossi, R. Cammi, B. Mennucci, C. Pomelli, C. Adamo, S. Clifford, J. Ochterski, G. Petersson, P. Ayala, Q. Cui, K. Morokuma, D. Malick, A. Rabuck, K. Raghavachari, J. Foresman, J. Cioslowski, J.V. Ortiz, A. Baboul, B. Stefanov, G. Liu, A. Liashenko, P. Piskorz, I. Komaromi, R. Gomperts, R. Martin, D. Fox, T. Keith, M. Al-Laham, C. Peng, A. Nanayakkara, C. Gonzalez, M. Challacombe, P. Gill, B. Johnson, W. Chen, M. Wong, J. Andres, C. Gonzalez, M. Head-Gordon, E. Replogle, J.P. And, *Gaussian 98, Revision A.7* (Gaussian Inc., Pittsburgh PA, 1998).
14. S. Boys, F. Bernardi, Mol. Phys. **19**, 533 (1970).
15. K.P. Huber, G. Herzberg, *Molecular spectra and molecular structure* (Van Nostrand Reinhold, N.Y., 1979).
16. W. Stwalley, W. Zemke, J. Phys. Chem. Ref. Data **22**, 87 (1993).
17. E. Bodo, F. Gianturco, F. Paesani, Z. Phys. Chem. **214**, 1013 (2000).
18. F.A. Gianturco, *The Transfer of Molecular Energies by Collision: Recent quantum treatments* (Springer Verlag, Berlin, 1979).
19. D.E. Manolopulos, J. Chem. Phys. **85**, 6425 (1986).
20. J.Z.H. Zhang, *Theory and application of quantum molecualr dynamics* (World Scientific, 1999).